# The Pulsed-Field Multiport Antenna System Reciprocity Relation and Its Applications—A Time-Domain Approach

Adrianus T. de Hoop, *Member, IEEE*, Ioan E. Lager, *Member, IEEE*, and Valerio Tomassetti

***Abstract*—A novel time-domain approach to the derivation of the pulsed electromagnetic field multiport antenna system reciprocity theorem is presented. The theorem interrelates the field and system properties in two states: the transmitting state and the receiving state. General time-domain Thévenin (voltage-source, impedance-based) and Norton (electric-current source, admittance-based) type equivalent circuits are constructed for antenna systems whose local properties are described in terms of multiport Kirchhoff circuits. Applications to an indoor wireless communication performance analysis and the analysis of cosmic microwave background radiation measurement are briefly indicated. Numerical results are provided for the pulsed-field transfer between two wire loops, a configuration that is representative for the operation of wireless telecommunication systems and for the pulsed-field EM interference analysis in nano-electronic integrated circuit devices.**

***Index Terms*—Antenna theory, equivalent circuit, reciprocity relation, time domain.**

## I. Introduction

RECIPROCITY relations belong to the basic tools of antenna system analysis. Through the relations, a number of fundamental antenna system properties can be established. In particular, a judicious application of reciprocity leads to the concept of an equivalent circuit that can be employed to account for the antenna system's operational behavior within the framework of a total (communication) system's analysis. Any reciprocity theorem interrelates the field, source and constitutive properties corresponding to two admissible 'states' in a time-invariant, linearly and causally reacting configuration. In antenna theory, the two states are any of the system's transmitting states and any of its receiving states, while the governing theorem involves electromagnetic fields, for which reciprocity has for the first time been discussed in a paper by H. A. Lorentz published in 1896 [1], [26]. In the majority of textbooks on electromagnetic theory (see, for example [2, Sec. 8.6–8.8], [3, pp. 49–50], [27], [28]), the theorem is formulated for and applied to time-harmonic fields, i.e., in the realm of a frequency-domain analysis. Reciprocity theorems pertaining to pulsed fields have been less discussed; in their general form they can be found in [4, Ch. 28]. In the recent literature, the transmitting/receiving reciprocity properties of antenna systems and the validity of their equivalent circuits have received renewed attention. Several aspects of the circuits are, still on the basis of a frequency-domain description, discussed in [5]–[8]. In view of the nowadays widespread use of pulsed signal communication (digital and ultrawideband), there is also a growing interest in the pulsed behavior of antenna systems and their transmitting/receiving properties [9]–[11]. An interesting development in this respect is the question of how to determine an 'optimum' pulse shape for the feed in a pulsed-operated antenna system such that at the receiving end a signal of a desired shape presents itself [12]. In all these studies, the time-domain reciprocity of antenna systems plays an instrumental role. While general references to electromagnetic time-domain reciprocity can be found in the literature (see, e.g., [4, Ch. 28], [13] and [14], [15]), the present work provides a comprehensive analysis of the specific relations characterizing multiport antenna systems, together with discussing some illustrative applications.

The general configuration that we consider is described in Section II. Section III presents the time-domain circuit description of the Kirchhoff port accessible antenna, both in the transmitting state and in the receiving state, for their Thévenin (voltage source, impedance-based) and Norton (electric-current source, admittance-based) representations. Section IV specifies the antenna circuit's reciprocity properties. Section V introduces the antenna's impulse-excited sensing fields in the transmitting state as they occur in the equivalent-circuit generator source strengths for incident radiation from known volume sources (Section VI) and for plane-wave incidence (Section VII). This reasoning runs parallel to the one employed in [16] for the frequency-domain analysis. Section VIII briefly discusses some applications: the design considerations of the antenna loading circuit, ingredients of an indoor wireless communication performance analysis, the interpretation of cosmic microwave background radiation measurement (where we introduce the concept of 'far-source approximation') and the wire loop as a receiving antenna. In Section IX, numerical results are presented for the pulsed-field transfer between two wire loops, a configuration that is representative for the operation of

Manuscript received October 31, 2007; revised November 12, 2008. Current version published March 27, 2009.

A. T. de Hoop is with the Laboratory of Electromagnetic Research, Faculty of Electrical Engineering, Mathematics and Computer Science, Delft University of Technology, 2628 CD Delft, The Netherlands (e-mail: a.t.dehoop@tudelft.nl).

I. E. Lager is with the International Research Centre for Telecommunications and Radar (IRCTR), Faculty of Electrical Engineering, Mathematics and Computer Science, Delft University of Technology, 2628 CD Delft, The Netherlands (e-mail: i.e.lager@tudelft.nl).

V. Tomassetti is with the Interuniversitary Master in Nanotechnologies, CIVEN, International Master Campus Villa Annia, 31056 Roncade (TV), Italy (e-mail: imntomasetti@civen.org).

Color versions of one or more of the figures in this paper are available online at http://ieeexplore.ieee.org.

Digital Object Identifier 10.1109/TAP.2009.2013422

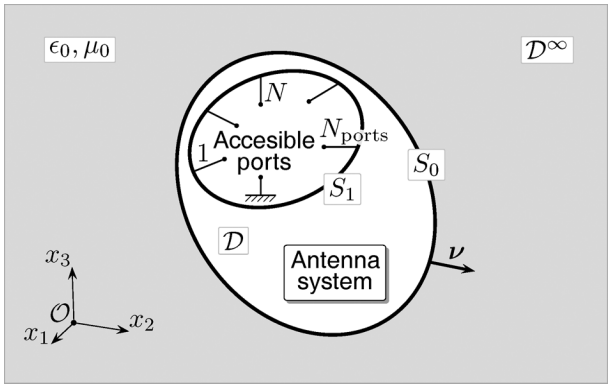


Fig. 1. Antenna configuration with $N_{\text{ports}}$ accessible Kirchhoff ports.

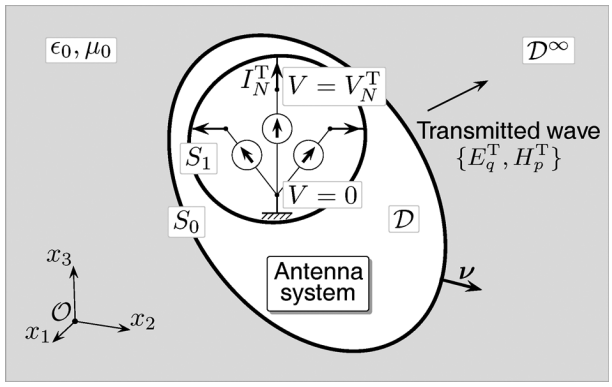


Fig. 2. Kirchhoff-type antenna in the transmitting situation; the accessible ports are fed by a multiport source.

wireless telecommunication systems and for the pulsed-field EM interference analysis in nano-electronic integrated circuit devices.

Appendix A presents the generic form of the field reciprocity theorem of the time-convolution type that we use. Appendix B shows the time-domain far-field representations. Appendix C gives the description of the receiving antenna as a scatterer in its embedding. Appendix D discusses the interfacing of the multiport Kirchhoff-type antenna system with the field description in its embedding.

## II. Description of the Configuration

The antenna system under consideration occupies a bounded domain in space $\mathcal{D}$. Externally, $\mathcal{D}$ is bounded by a sufficiently regular, closed surface $\mathcal{S}_0$, and internally it is bounded by a sufficiently regular, closed surface $\mathcal{S}_1$. The surface $\mathcal{S}_1$ is considered as the termination of the antenna system, and on it the antenna system terminates into $N_{\text{ports}}$ accessible ports (see Fig. 1). The other parts of the antenna structure are located in between $\mathcal{S}_1$ and $\mathcal{S}_0$. Parts of $\mathcal{S}_0$ and $\mathcal{S}_1$ may coincide. The region $\mathcal{D}$ thus introduced allows us to distinguish the antenna system from the environment into which it radiates or scatters, that we will indicate by $\mathcal{D}^\infty$, as well as from the ports at which it is accessible.

Position in the configuration is specified by the coordinates $\{x_1, x_2, x_3\}$ with respect to an orthogonal Cartesian reference frame with the origin $\mathcal{O}$ and the three mutually perpendicular base vectors $\{\boldsymbol{i}_1, \boldsymbol{i}_2, \boldsymbol{i}_3\}$ of unit length each. In the indicated order, the base vectors form a right-handed system. The subscript notation for Cartesian vectors and tensors is used and the summation convention for repeated subscripts applies [4]; lower-case Latin symbols are used to this purpose. Whenever appropriate, vectors are indicated by boldface symbols, with $\boldsymbol{x}$ as the position vector. The time coordinate is $t$. Partial differentiation with respect to $x_m$ will be denoted by $\partial_m$; $\partial_t$ is a reserved symbol indicating partial differentiation with respect to $t$. Time convolution will be denoted by the symbol $\overset{(t)}{*}$. The superscripts T and R are used to denote the transmitting and the receiving states, respectively.

The antenna configuration consists of a medium, the electromagnetic behavior of which is linear, passive, time-invariant and causal. No further restrictions as to its electromagnetic properties are imposed. In particular, the cases of anisotropy, inhomogeneity and arbitrary loss mechanisms are explicitly accounted for. The properties of the medium are allowed to change abruptly upon crossing a (bounded) surface. The configuration may also contain parts that are perfectly conducting. The medium outside $\mathcal{S}_0$ is assumed to be linear, homogeneous, isotopic and lossless, with real scalar electric permittivity $\epsilon_0 > 0$ and magnetic permeability $\mu_0 > 0$.

## III. The General Time-Domain Circuit Description of the Kirchhoff-Type Antenna

Let the antenna system be accessible via $N_{\text{ports}}$ ($N_{\text{ports}} \geqslant 1$) Kirchhoff ports (see Fig. 2). Let $I_N^{\text{T}}(t)$ denote the electric current fed into the $N$th port and let $V_N^{\text{T}}(t)$ denote the voltage across the $N$th port ($N = 1, \ldots, N_{\text{ports}}$). As a consequence of the uniqueness theorem of electromagnetic fields, the voltages $V_N^{\text{T}}(t)$ in the transmitting state T are linearly related to the associated currents $I_N^{\text{T}}(t)$ through a relation of the type

$$V_M^{\text{T}}(t) = \sum_{N=1}^{N_{\text{ports}}} Z_{M,N}^{\text{in}}(t) \overset{(t)}{*} I_N^{\text{T}}(t) \quad \text{for} \quad M = 1, \ldots, N_{\text{ports}} \tag{1}$$

where $Z_{M,N}^{\text{in}}(t)$ represents the causal, time-domain input impedance matrix of the radiating system in the transmitting situation. Equivalently, a relation of the type

$$I_N^{\text{T}}(t) = \sum_{M=1}^{N_{\text{ports}}} Y_{N,M}^{\text{in}}(t) \overset{(t)}{*} V_M^{\text{T}}(t) \quad \text{for} \quad N = 1, \ldots, N_{\text{ports}} \tag{2}$$

holds, where $Y_{N,M}^{\text{in}}(t)$ represents the causal, time-domain input admittance matrix of the radiating system in the transmitting situation. Obviously, the input impedance matrix and the input admittance matrix are each others' inverses.

Through the application of the reciprocity relation (53) it will be shown that, in the receiving situation, the signal behavior of the antenna system can be described by a relation of the type (Thévenin description)

$$V_M^{\text{R}}(t) + \sum_{N=1}^{N_{\text{ports}}} Z_{M,N}^{\text{in}}(t) \overset{(t)}{*} I_N^{\text{R}}(t) = V_{M^{\text{G}}}(t) \quad \text{for} \quad M = 1, \ldots, N_{\text{ports}} \tag{3}$$

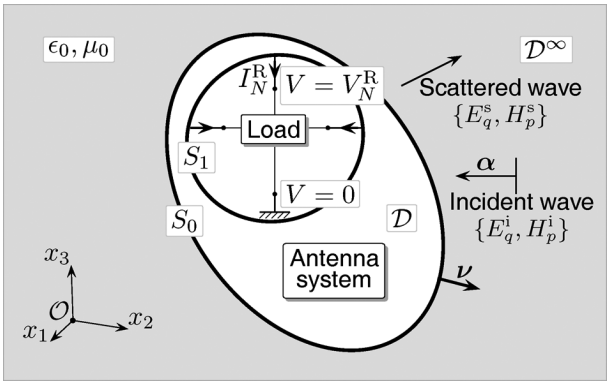


Fig. 3. Loaded Kirchhoff-type antenna in the receiving state for plane, electromagnetic pulse incidence.

in which the "Thévenin equivalent generator voltage" $V_M^{\mathrm{G}}(t)$ is related to the incident field, or, equivalently, by a relation of the type (Norton description)

$$I_N^{\mathrm{R}}(t) + \sum_{M=1}^{N_{\mathrm{ports}}} Y_{N,M}^{\mathrm{in}}(t) \overset{(t)}{*} V_M^{\mathrm{R}}(t) = I_N^{\mathrm{G}}(t) \quad \text{for} \quad N = 1, \ldots, N_{\mathrm{ports}} \tag{4}$$

in which, now, the 'Norton equivalent generator current' $I_N^{\mathrm{G}}(t)$ is related to the incident field. Note that, to comply with the customary convention in circuit theory, the electric currents in the receiving situation are oriented *into* the load (see Fig. 3). To determine from (3) and (4) the actual pulse shapes of the circuit quantities in the actual operation of the system, these relations have to be supplemented with the time-domain loading conditions of the type

$$V_M^{\mathrm{R}}(t) = \sum_{N=1}^{N_{\mathrm{ports}}} Z_{M,N}^{\mathrm{L}}(t) \overset{(t)}{*} I_N^{\mathrm{R}}(t) \quad \text{for} \quad M = 1, \ldots, N_{\mathrm{ports}} \tag{5}$$

where $Z_{M,N}^{\mathrm{L}}(t)$ are the elements of a passive load impedance matrix or

$$I_N^{\mathrm{R}}(t) = \sum_{M=1}^{N_{\mathrm{ports}}} Y_{N,M}^{\mathrm{L}}(t) \overset{(t)}{*} V_M^{\mathrm{R}}(t) \quad \text{for} \quad N = 1, \ldots, N_{\mathrm{ports}} \tag{6}$$

where $Y_{N,M}^{\mathrm{L}}(t)$ are the elements of a passive load admittance matrix. Once the properties of the antenna system in the transmitting situation are known, its properties in the receiving situation follow as soon as the generator source terms in (3) and (4) have been determined and the loading conditions have been specified.

It is of importance to note that, as will be shown in (3) and (4), the actual input impedance and admittance matrices from (1) and (2) occur, even if, for the case of anisotropy, the medium properties are non-reciprocal.

In the equivalent circuit relations, time convolution operators occur, as could be expected, at those positions where mere multiplications occur in their frequency-domain counterparts (as, for example, those provided in [16]).

## IV. Time-Domain Antenna Circuit Reciprocity

A first property of the antenna input impedance and admittance matrices is that, upon changing the medium properties in the configuration into their adjoint ones, these matrix operators change into their transposed ones. To prove this, the generic form of the source-free counterpart of the time-domain reciprocity relation (53) is applied to the domain bounded internally by $\mathcal{S}_1$ and externally by the sphere $\mathcal{S}_r$ of radius $r$ and center at the reference center of the antenna, using on $\mathcal{S}_r$ the relevant far-field representations (56) and taking the limit $r \to \infty$, while employing on $\mathcal{S}_1$ the field/circuit interfacing relation (64). Substituting in the result the relations (1) and (2) applying to the two states, it follows that [cf. (49) and (50)] for

$$\left\{\eta_{k,q}^{\mathrm{B}}, \zeta_{j,p}^{\mathrm{B}}\right\}(\boldsymbol{x}, t) = \left\{\eta_{q,k}^{\mathrm{A}}, \zeta_{p,j}^{\mathrm{A}}\right\}(\boldsymbol{x}, t) \tag{7}$$

we have

$$\left\{Z_{M,N}^{\mathrm{B}}, Y_{N,M}^{\mathrm{B}}\right\}(t) = \left\{Z_{N,M}^{\mathrm{A}}, Y_{M,N}^{\mathrm{A}}\right\}(t) \tag{8}$$

which is the desired relation.

## V. The Antenna's Impulse Excited Sensing Field Constituents

In the generator source strengths of the equivalent circuits representing the antenna's behavior in the receiving situation, the antenna's impulse excited sensing field constituents in its transmitting state will occur. These field constituents follow from the linear relationship between the transmitted field in the antenna's embedding on the one hand and the exciting voltages in the Thévenin description and the exciting electric currents in the Norton description on the other hand. We write

$$\left\{E_q^{\mathrm{T}}, H_p^{\mathrm{T}}\right\} = \sum_{N=1}^{N_{\mathrm{ports}}} \left\{E_q^{\mathrm{T}}\big|_{I_N^{\mathrm{T}}=\delta(t)}, H_p^{\mathrm{T}}\big|_{I_N^{\mathrm{T}}=\delta(t)}\right\} \overset{(t)}{*} I_N^{\mathrm{T}} \tag{9}$$

that will occur in the generator voltage source strengths in the Thévenin receiving circuit and

$$\left\{E_q^{\mathrm{T}}, H_p^{\mathrm{T}}\right\} = \sum_{M=1}^{N_{\mathrm{ports}}} \left\{E_q^{\mathrm{T}}\big|_{V_M^{\mathrm{T}}=\delta(t)}, H_p^{\mathrm{T}}\big|_{V_M^{\mathrm{T}}=\delta(t)}\right\} \overset{(t)}{*} V_M^{\mathrm{T}} \tag{10}$$

that will occur in the generator electric current source strengths in the Norton receiving circuit. Note that these impulse excited field constituents are *configurational* parameters characterizing the antenna's field emission into the embedding.

## VI. The Equivalent-Circuit Generator Source Strengths for Incident Radiation From Known Volume Source Distributions

In a typical telecommunications environment, the sensitivity of a receiving antenna to an incident field that arises from the action of known volume sources elsewhere, is a factor

of importance in the overall characterization of the system. To analyze this situation, the generic form of the time-domain reciprocity relation (53) is applied to the transmitting state T and the receiving state R and the domain bounded internally by $\mathcal{S}_1$ and externally by the sphere $\mathcal{S}_r$ of radius $r$ and center at the reference center of the antenna. Using $\{J_k^{\mathrm{T}}, K_j^{\mathrm{T}}\} = \{0, 0\}$ in the relevant domain integral, choosing $\{\eta_{k,q}^R, \zeta_{j,p}^R\}(\boldsymbol{x}, t) = \{\eta_{q,k}^T, \zeta_{p,j}^T\}(\boldsymbol{x}, t)$, taking into account that in both states the fields admit, on $\mathcal{S}_r$, far-field representations of the type (56), taking the limit $r \to \infty$ and employing on $\mathcal{S}_1$ the field/circuit interfacing relation (64), it follows that

$$\sum_{M=1}^{N_{\mathrm{ports}}} V_M^{\mathrm{T}}(t) \overset{(t)}{*} I_M^{\mathrm{R}}(t) + \sum_{N=1}^{N_{\mathrm{ports}}} V_N^{\mathrm{R}}(t) \overset{(t)}{*} I_N^{\mathrm{T}}(t) = \int_{\mathcal{D}^{\mathrm{R}}} \left( -J_k^{\mathrm{R}} \overset{(t)}{*} E_k^{\mathrm{T}} + K_j^{\mathrm{R}} \overset{(t)}{*} H_j^{\mathrm{T}} \right) \mathrm{d}V(\boldsymbol{x}) \quad (11)$$

where $\mathcal{D}^{\mathrm{R}}$ is the spatial support of the volume source distributions.

### A. The Thévenin (Voltage Source) Equivalent Circuit

To arrive at the expression for the generator voltage source strength in the Thévenin equivalent circuit, we substitute in (11) the relation (1) and use (9). Observing that the resulting relation has to hold for arbitrary values of $I_N^{\mathrm{T}}$ and using (8), we end up with (3) in which

$$V_N^{\mathrm{G}}(t) = \int_{\mathcal{D}^{\mathrm{R}}} \left[ -E_k^{\mathrm{T}}\big|_{I_N(t)=\delta(t)} \overset{(t)}{*} J_k^{\mathrm{R}} + H_j^{\mathrm{T}}\big|_{I_N(t)=\delta(t)} \overset{(t)}{*} K_j^{\mathrm{R}} \right] \mathrm{d}V. \quad (12)$$

### B. The Norton (Electric-Current Source) Equivalent Circuit

To arrive at the expression for the generator electric current source strength in the Norton equivalent circuit, we substitute in (11) the relation (2) and use (10). Observing that the resulting relation has to hold for arbitrary values of $V_M^{\mathrm{T}}$ and using (8), we end up with (4) in which

$$I_M^{\mathrm{G}}(t) = \int_{\mathcal{D}^{\mathrm{R}}} \left[ -E_k^{\mathrm{T}}\big|_{V_M(t)=\delta(t)} \overset{(t)}{*} J_k^{\mathrm{R}} + H_j^{\mathrm{T}}\big|_{V_M(t)=\delta(t)} \overset{(t)}{*} K_j^{\mathrm{R}} \right] \mathrm{d}V. \quad (13)$$

## VII. The Equivalent-Circuit Generator Source Strengths for Plane Wave Incidence

In radar and other remote-sensing applications, the field intercepted by the antenna system in the receiving state can, to a sufficient degree of accuracy, be described as a uniform plane wave. A factor of importance in the overall characterization of the system is then the antenna's sensitivity in dependence on the pulse amplitude, the pulse shape, the state of polarization and direction of incidence of the wave. Although this situation could be handled via a limiting procedure of the case described in Section VI by letting the generating sources recede to infinity, a much easier procedure to arrive at expressions for the generator source strengths in the equivalent circuits is to use a scattering description and employ the surface source expressions discussed in Appendix B. Let the incident wave be specified as

$$\{E_q^{\mathrm{i}}, H_p^{\mathrm{i}}\} = \{e_q^{\mathrm{i}}, h_p^{\mathrm{i}}\}\, a(t - \alpha_s x_s / c_0) \quad (14)$$

where $\alpha_s$ (with $\alpha_s \alpha_s = 1$) denotes the unit vector in the direction of propagation, $\{e_q^{\mathrm{i}}, h_p^{\mathrm{i}}\}$ are the polarization vectors of the fields and $a(t)$ is the (somehow normalized) pulse shape of the wave motion. Upon substituting (14) in the sourcefree counterparts of the Maxwell (47) and (48), supplemented with the free-space constitutive relations (51) and (52), it follows that

$$e_q^{\mathrm{i}} = -(\mu_0/\epsilon_0)^{1/2} \varepsilon_{q,n,p} \alpha_n h_p^{\mathrm{i}} \quad (15)$$

$$h_p^{\mathrm{i}} = (\epsilon_0/\mu_0)^{1/2} \varepsilon_{p,n,q} \alpha_n e_q^{\mathrm{i}} \quad (16)$$

The total received field can be taken as the superposition of the incident $\{E_q^{\mathrm{i}}, H_p^{\mathrm{i}}\}$ and the scattered $\{E_q^{\mathrm{s}}, H_p^{\mathrm{s}}\}$ fields, i.e.,

$$\{E_q^{\mathrm{R}}, H_p^{\mathrm{R}}\} = \{E_q^{\mathrm{i}} + E_q^{\mathrm{s}}, H_p^{\mathrm{i}} + H_p^{\mathrm{s}}\}. \quad (17)$$

To handle this case (note that the incident plane wave does not satisfy the radiation condition) the generic form of the time-domain reciprocity relation (53) is applied to the transmitting state T and the scattering state s, and the sourcefree domain bounded internally by $\mathcal{S}_0$ and externally by the sphere $\mathcal{S}_r$ of radius $r$ and center at the reference center of the antenna. Both, the transmitted field and the scattered field admit far-field representations of the type (56) and, hence the contribution from $\mathcal{S}_r$ vanishes in the limit $r \to \infty$. Consequently, applying (53) to the source-free externally unbounded domain that is bounded internally by $\mathcal{S}_0$, it then follows that

$$\varepsilon_{k,m,p} \int_{\mathcal{S}_0} \nu_k \left( E_m^{\mathrm{T}} \overset{(t)}{*} H_p^{\mathrm{s}} - E_m^{\mathrm{s}} \overset{(t)}{*} H_p^{\mathrm{T}} \right) \mathrm{d}A(\boldsymbol{x}) = 0. \quad (18)$$

By invoking the surface-source representation for the far-field scattered wave amplitude following from Appendix B, it can be established that [4, p. 891]

$$\varepsilon_{k,m,p} \int_{\mathcal{S}_0} \nu_k \left( E_m^{\mathrm{T}} \overset{(t)}{*} H_p^{\mathrm{i}} - E_m^{\mathrm{i}} \overset{(t)}{*} H_p^{\mathrm{T}} \right) \mathrm{d}A(\boldsymbol{x}') = -\mu_0^{-1} E_q^{\mathrm{i}}(t) \overset{(t)}{*} \mathbf{I}_t \left[ E_q^{\mathrm{T},\infty}(-\boldsymbol{\alpha}, t) \right] \quad (19)$$

where $\mathbf{I}_t$ denotes the time integration operator, defined through

$$\mathbf{I}_t [f(\boldsymbol{x}, t)] = \int_{t'=-\infty}^{t} f(\boldsymbol{x}, t') \mathrm{d}t'. \quad (20)$$

Combining (18) and (19) with (17) we obtain

$$\varepsilon_{k,m,p} \int_{\mathcal{S}_0} \nu_k \left( E_m^{\mathrm{T}} \overset{(t)}{*} H_p^{\mathrm{R}} - E_m^{\mathrm{R}} \overset{(t)}{*} H_p^{\mathrm{T}} \right) \mathrm{d}A(\boldsymbol{x}) = -\mu_0^{-1} E_q^{\mathrm{i}}(t) \overset{(t)}{*} \mathbf{I}_t \left[ E_q^{\mathrm{T},\infty}(-\boldsymbol{\alpha}, t) \right]. \quad (21)$$

Finally, applying (53) to the domain bounded internally by $\mathcal{S}_1$ and externally by $\mathcal{S}_0$ and the states T and R, we obtain

$$\varepsilon_{k,m,p}\int_{\mathcal{S}_0}\nu_k\left(E_m^{\mathrm{T}}\overset{(t)}{*}H_p^{\mathrm{R}}-E_m^{\mathrm{R}}\overset{(t)}{*}H_p^{\mathrm{T}}\right)\mathrm{d}A(\boldsymbol{x})$$
$$=\varepsilon_{k,m,p}\int_{\mathcal{S}_1}\nu_k\left(E_m^{\mathrm{T}}\overset{(t)}{*}H_p^{\mathrm{R}}-E_m^{\mathrm{R}}\overset{(t)}{*}H_p^{\mathrm{T}}\right)\mathrm{d}A(\boldsymbol{x}). \quad (22)$$

With the aid of the field/circuit interfacing relation (64) on $\mathcal{S}_1$ it then follows that

$$\sum_{M=1}^{N_{\mathrm{ports}}}V_M^{\mathrm{T}}(t)\overset{(t)}{*}I_M^{\mathrm{R}}(t)+\sum_{N=1}^{N_{\mathrm{ports}}}V_N^{\mathrm{R}}(t)\overset{(t)}{*}I_N^{\mathrm{T}}(t)$$
$$=-\mu_0^{-1}E_q^{\mathrm{i}}(t)\overset{(t)}{*}\mathbf{I}_t\left[E_q^{\mathrm{T},\infty}(-\boldsymbol{\alpha},t)\right]. \quad (23)$$

### A. The Thévenin (Voltage Source) Equivalent Circuit

To arrive at the expression for the generator voltage source strength in the Thévenin equivalent circuit, we substitute in (23) the relation (1) and use (9). Observing that the resulting relation has to hold for arbitrary values of $I_N^{\mathrm{T}}$ and using (8), we end up with (3) in which

$$V_N^{\mathrm{G}}(t)=-\mu_0^{-1}e_q^{\mathrm{i}}\mathbf{I}_t a(t)\overset{(t)}{*}\left[E_q^{\mathrm{T},\infty}\big|_{I_N^{\mathrm{T}}=\delta(t)}(-\boldsymbol{\alpha},t)\right]$$
$$\text{for}\quad N=1,\ldots,N_{\mathrm{ports}}. \quad (24)$$

### B. The Norton (Electric-Current Source) Equivalent Circuit

To arrive at the expression for the generator electric current source strength in the Norton equivalent circuit, we substitute in (23) the relations (2) and use (10). Observing that the resulting relation has to hold for arbitrary values of $V_M^{\mathrm{T}}$ and using (8), we end up with (4) in which

$$I_M^{\mathrm{G}}(t)=-\mu_0^{-1}e_q^{\mathrm{i}}\mathbf{I}_t a(t)\overset{(t)}{*}\left[E_q^{\mathrm{T},\infty}\big|_{V_M^{\mathrm{T}}=\delta(t)}(-\boldsymbol{\alpha},t)\right]$$
$$\text{for}\quad M=1,\ldots,N_{\mathrm{ports}}. \quad (25)$$

Note that in (24) and (25) the antenna's impulse excited far-field region sensing fields occur, taken in the direction from which the plane wave is incident and that the latter's time-integrated pulse shape is involved.

## VIII. Applications

In this section, a variety of applications of the reciprocity relation will be discussed. They include: (A) certain design considerations as regards the antenna loading circuit, (B) how the reciprocity relations are applicable to a typical indoor wireless communication system performance analysis, (C) the interpretation of cosmic microwave background radiation measurement (where the concept of 'far-source approximation' is introduced), (D) the action of the wire loop as a receiving antenna, which case is, although elementary, the basic ingredient of the pulsed-field electromagnetic interference analysis of all electric and electronic circuits.

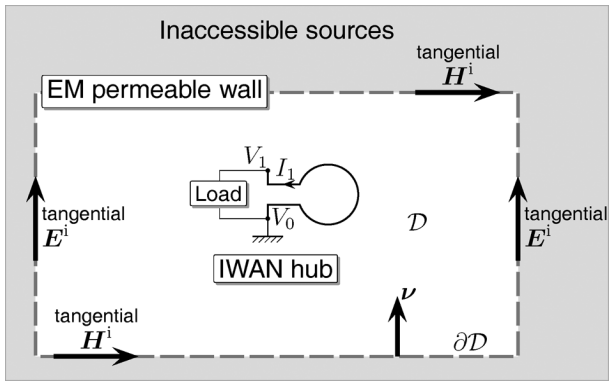


Fig. 4. Operation of an IWAN hub under the influence of an incoming field that penetrates through the walls of the indoor scenario.

### A. Design Considerations of the Antenna Loading Circuit

The equivalent circuits obtained provide the basis for further designing loading circuits that are specified by (5) and (6) and are to perform certain actions on the received signals. All circuit relations involved are of the time-convolution type. So, for example, Wiener filtering can be applied to minimize the signal distortion due to the presence of noise via the application of the Wiener-Hopf technique [17, p. 397]. Another interesting development is the research into optimizing the transmitted pulse shape of the antenna to given loading conditions, as discussed, for a simple example, in [12].

### B. Application to Indoor Wireless Communication Performance Analysis

Recently, many gigahertz of bandwidth have been authorized for license-free wireless personal area networks (WPANs) making use of ultrawideband signals (see [18] for the relevant spectrum allocation). A typical application of this kind concerns the intelligent wireless area networks (IWAN), of which Fig. 4 is illustrative for the corresponding indoor communication scenario described in [19].

A general performance analysis, aimed at the reception capabilities of signals generated elsewhere, as well as aimed at an immunity analysis against incoming disturbances, is readily carried out by applying (63) to the room $\mathcal{D}$ where operation is planned and its bounding wall $\partial\mathcal{D}$. In both cases, the scattering analysis of Appendix C is used, the external sources generating the incident field being located outside $\mathcal{D}$. Proceeding as in Section VI, we end up with (3) in which

$$V_N^{\mathrm{G}}(t)=\varepsilon_{k,m,p}\int_{\partial\mathcal{D}}\nu_k\left[E_m^{\mathrm{T}}\big|_{I_N^{\mathrm{T}}=\delta(t)}\overset{(t)}{*}H_p^{\mathrm{i}}\right.$$
$$\left.-E_m^{\mathrm{i}}\big|_{I_N^{\mathrm{T}}=\delta(t)}\overset{(t)}{*}H_p^{\mathrm{T}}\right]\mathrm{d}A(\boldsymbol{x})\ \text{ for }\ N=1,\ldots,N_{\mathrm{ports}} \quad (26)$$

or with (4), in which

$$I_M^{\mathrm{G}}(t)=\varepsilon_{k,m,p}\int_{\partial\mathcal{D}}\nu_k\left[E_m^{\mathrm{T}}\big|_{V_M^{\mathrm{T}}=\delta(t)}\overset{(t)}{*}H_p^{\mathrm{i}}\right.$$
$$\left.-E_m^{\mathrm{i}}\big|_{V_M^{\mathrm{T}}=\delta(t)}\overset{(t)}{*}H_p^{\mathrm{T}}\right]\mathrm{d}A(\boldsymbol{x})\ \text{ for }\ M=1,\ldots,N_{\mathrm{ports}}. \quad (27)$$

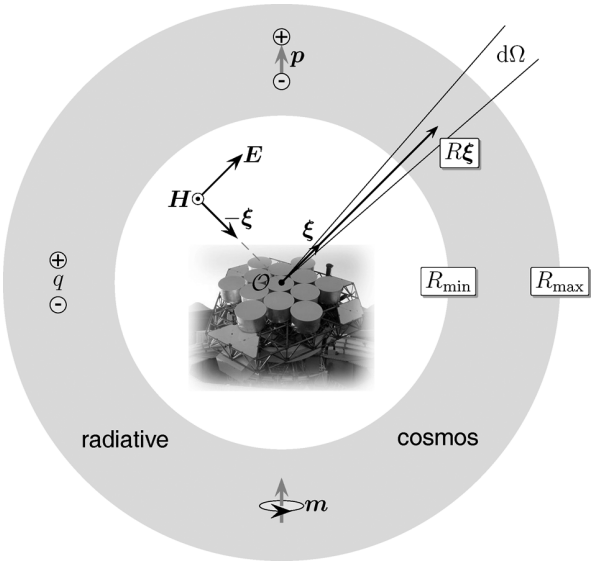


Fig. 5. Radiative cosmos with moving electric charges, electric dipoles and magnetic (spin) dipoles, and observation coordinates for the measurement of CMB radiation. The picture in the center depicts the Caltech Cosmic Background Imager, freely downloadable from http://www.astro.caltech.edu/~tjp/CBI/press2/index.html.

As these expression show, the action of the "electromagnetic environment" on the performance of a receiving antenna system placed anywhere in $\mathcal{D}$ is fully specified by the values of the tangential electric and magnetic field strengths on the wall $\partial\mathcal{D}$ of the room at which they are accessible to measurement. Note that the unit vector normal to the boundary is oriented towards $\mathcal{D}$. The expressions are also a convenient starting point for a statistical performance analysis, where the reception properties of the antenna are determined by the statistical properties of the incident field.

### C. Application to Cosmic Microwave Background Radiation Measurement Interpretation. The Far-Source Approximation

Fig. 5 represents a typical cosmic microwave background (CMB) radiation measurement configuration (as the one described in [20]). Here, the reciprocity theorem serves to express the equivalent-circuit generator source strengths in terms of the cosmic volume source distributions that are conjectured to generate the radiation, viz. the volume density of electric convection current $J_k$ associated with the freely moving electrically charged particles, the volume source density of electric polarization $P_k$ associated with the oscillations of atomic electric dipoles and the volume source density of magnetization $M_j$ associated with the orientation changing atomic magnetic spins in the far regions of the cosmos.

Application of (53) to the entire domain exterior to the bounding surface of the Kirchhoff ports yields (12) and (13) with $J_k^{\mathrm{R}} = J_k + \partial_t P_k$ and $K_j^{\mathrm{R}} = \partial_t M_j$.

In view of the large (cosmic) transmission paths involved, the field values of the impulse-excited sensing fields in the transmission state can, in the radiative cosmos, be replaced by their far-field approximations (see Appendix B). Introducing the radial distance $R$ from the antenna reference center to the radiating cosmic source distribution and the unit vector $\boldsymbol{\xi}$ in the radial direction as the variables of integration and only retaining the terms that vary as $R^{-1}$ with increasing $R$, we obtain the *far-source approximations* as in (28), shown at the bottom of the page, for the use in (3) and (29), shown at the bottom of the page, for the use in (4), where $\Omega$ is the unit sphere and the spherical shell to be sensed is of inner radius $R_{\min}$ and outer radius $R_{\max}$.

As (28) and (29) show, the integral with respect to $R$ consists of the contributions from spherical shells that are the "far-source" counterparts of the "slant-stack" contributions occurring in the customary far-field representation [13]. To arrive at the reconstruction of the cosmic radiative source distributions as those reported in [22], the measured signals at the accessible ports of the receiving antenna are subjected to the techniques of solving inverse source problems [21].

### D. The Wire Loop as a Receiving Antenna

In this subsection, we consider the receiving properties of a single wire loop in free space, immersed in a pulsed incident field $\{E_q^i, H_p^i\}$. This configuration can be considered as generic

$$V_N^{\mathrm{G}} \simeq \frac{1}{4\pi}\int_{\boldsymbol{\xi}\in\Omega} \mathrm{d}\Omega \left( \int_{R=R_{\min}}^{R_{\max}} R\mathrm{d}R \left\{ -E_k^{\mathrm{T};\infty}|_{I_N(t)=\delta(t)}(\boldsymbol{\xi}, t-R/c_0) \overset{(t)}{*} [J_k(R\boldsymbol{\xi},t) + \partial_t P_k(R\boldsymbol{\xi},t)] \right.\right.$$
$$\left.\left. + H_j^{\mathrm{T};\infty}|_{I_N(t)=\delta(t)}(\boldsymbol{\xi}, t-R/c_0) \overset{(t)}{*} \partial_t M_j(R\boldsymbol{\xi},t) \right\}\right) \quad (28)$$

$$I_M^{\mathrm{G}} \simeq \frac{1}{4\pi}\int_{\boldsymbol{\xi}\in\Omega} \mathrm{d}\Omega \left( \int_{R=R_{\min}}^{R_{\max}} R\mathrm{d}R \left\{ -E_k^{\mathrm{T};\infty}|_{V_M(t)=\delta(t)}(\boldsymbol{\xi}, t-R/c_0) \overset{(t)}{*} [J_k(R\boldsymbol{\xi},t) + \partial_t P_k(R\boldsymbol{\xi},t)] \right.\right.$$
$$\left.\left. + H_j^{\mathrm{T};\infty}|_{V_M(t)=\delta(t)}(\boldsymbol{\xi}, t-R/c_0) \overset{(t)}{*} \partial_t M_j(R\boldsymbol{\xi},t) \right\}\right) \quad (29)$$

to the large class of electrical or electronic devices whose topology consists of a collection of interconnected loops to which Kirchhoff voltage and electric current laws apply. Let $\mathcal{L}$ be the center line of the loop and let the loop be accessible at a single port with terminal voltage $V(t)$ and electric current $I(t)$. We shall present the details for the Thévenin circuit representation.

In the transmitting state, (1) reduces to

$$V^{\mathrm{T}}(t) = Z^{\mathrm{in}}(t) \overset{(t)}{*} I^{\mathrm{T}}(t). \tag{30}$$

Using the scattering description of Appendix C, evaluating the reciprocity interaction integral over the boundary surface of the loop, neglecting the electric field in the interior of the conducting loop, taking into account the relation between the value of the magnetic field on the surface of the loop and the thin-wire axial electric current flowing in its interior (Ampere's law) we end up with

$$V^{\mathrm{G}}(t) = \int_{\mathcal{L}^{\mathrm{R}}} E^i_k \tau_k \mathrm{d}s \tag{31}$$

where $\tau_k$ is the unit vector along the tangent of $\mathcal{L}^{\mathrm{R}}$, oriented in conformity with the orientation of $I(t)$ at the accessible port. Application of Faraday's induction law leads to the final expression

$$V^{\mathrm{G}}(t) = -\mu_0 \partial_t \int_{\mathcal{S}_{\mathcal{L}^{\mathrm{R}}}} H^i_j \nu_j \mathrm{d}A \tag{32}$$

where $\mathcal{S}_{\mathcal{L}^{\mathrm{R}}}$ is some two-sided surface with $\mathcal{L}^{\mathrm{R}}$ as boundary and $\nu_j$ is the unit vector along the normal to $\mathcal{S}_{\mathcal{L}^{\mathrm{R}}}$ in a right-handed manner related to $\tau_k$. As (32) shows, the pulse shape of the generator voltage source is the time derivative of the one of the local incident magnetic field. Note that, through the use of the scattering description in the reciprocity relation, it has rigorously been shown that in the right-hand side the *incident* magnetic field occurs and not the *total* one.

For a sufficiently small loop, (32) can be approximated by

$$V^{\mathrm{G}}(t) \simeq -\mu_0 \partial_t H^i_j(\boldsymbol{x}^{\mathrm{R}}, t) A^{\mathrm{R}}_j \tag{33}$$

where $\boldsymbol{x}^{\mathrm{R}}$ is the antenna reference center of the loop and

$$A^{\mathrm{R}}_j = \int_{\mathcal{S}_{\mathcal{L}^{\mathrm{R}}}} \nu_j \mathrm{d}A \tag{34}$$

is the vectorial area of the loop.

## IX. Numerical Results for the Pulse Shape Variation With Distance and Orientation in a Two Wire-Loop Field Transfer System

In this section we illustrate how the generator source voltage $V^{\mathrm{G}}(t)$ in the equivalent Thévenin circuit of a receiving loop $\mathcal{L}^{\mathrm{R}}$ varies with distance and orientation in case the loop is placed in the field emitted by another (transmitting) loop $\mathcal{L}^{\mathrm{T}}$ that is activated by an electric current pulse $I^{\mathrm{T}}(t)$. The activating current pulse is characterized by its amplitude $I_{\max}$, its pulse rise time $t_{\mathrm{r}}$ and its pulse time width $t_{\mathrm{w}}$. For the pulse shape we take the *power exponential pulse* [23]

$$I^{\mathrm{T}}(t) = I^{\mathrm{T}}_{\max} (t/t_{\mathrm{r}})^{\nu} \exp\left[-\nu(t/t_{\mathrm{r}}) + \nu\right] H(t) \tag{35}$$

with power $\nu$ that is related to $t_{\mathrm{r}}$ and $t_{\mathrm{w}}$ via

$$t_{\mathrm{w}} = \Gamma(\nu+1) \frac{\exp(\nu)}{\nu^{\nu+1}} t_{\mathrm{r}} \tag{36}$$

with $\Gamma$ denoting the Euler gamma function, and $H(t)$ as the Heaviside unit step function. The magnetic field emitted by the loop observed at the vectorial position $\boldsymbol{X} = \boldsymbol{x}^{\mathrm{R}} - \boldsymbol{x}^{\mathrm{T}}$ with respect to the reference center of $\mathcal{L}^{\mathrm{T}}$ is given by [4, p. 761]

$$\begin{aligned} H^{\mathrm{T}}_j(\boldsymbol{X}, t) = \Bigg[ & D^{\mathrm{NF}}_{j,p}(\boldsymbol{\Xi}) \frac{I^{\mathrm{T}}\left(t - |\boldsymbol{x}|/c_0\right)}{4\pi |\boldsymbol{X}|^3} \\ & + D^{\mathrm{IF}}_{j,p}(\boldsymbol{\Xi}) \frac{c_0^{-1} \partial_t I^{\mathrm{T}}\left(t - |\boldsymbol{X}|/c_0\right)}{4\pi |\boldsymbol{X}|^2} \\ & + D^{\mathrm{FF}}_{j,p}(\boldsymbol{\Xi}) \frac{c_0^{-2} \partial_t^2 I^{\mathrm{T}}\left(t - |\boldsymbol{X}|/c_0\right)}{4\pi |\boldsymbol{X}|} \Bigg] A^{\mathrm{T}}_p \end{aligned} \tag{37}$$

where

$$D^{\mathrm{NF}}_{j,p}(\boldsymbol{\Xi}) = D^{\mathrm{IF}}_{j,p}(\boldsymbol{\Xi}) = 3\Xi_j \Xi_p - \delta_{j,p} \tag{38}$$

are the near-field (NF) and intermediate-field (IF) direction characteristics,

$$D^{\mathrm{FF}}_{j,p}(\boldsymbol{\Xi}) = \Xi_j \Xi_p - \delta_{j,p} \tag{39}$$

is the far-field (FF) direction characteristic, and $A^{\mathrm{T}}_p$ is the vectorial area of the transmitting loop. In (38) and (39), $\Xi_p = X_p/|\boldsymbol{X}|$ is the unit vector along $\boldsymbol{X}$ and $\delta_{j,p}$ is the Kronecker tensor: $\delta_{j,p} = 1$ for $j = p$, $\delta_{j,p} = 0$ for $j \neq p$. Substitution of (37) in (33) then yields the generator voltage in the equivalent circuit of the receiving loop

$$V^{\mathrm{G}}(t) \simeq -\mu_0 \partial_t H^{\mathrm{T}}_j(\boldsymbol{X}, t) A^{\mathrm{R}}_j. \tag{40}$$

For plotting purposes, a normalized counterpart $V^{\mathrm{G}}_{\mathrm{norm}}(t)$ of $V^{\mathrm{G}}(t)$ will be employed, defined as

$$V^{\mathrm{G}}_{\mathrm{norm}}(t) = -\left[ \left( \frac{\mu_0}{\epsilon_0} \right)^{1/2} I^{\mathrm{T}}_{\max} \frac{A^{\mathrm{R}} A^{\mathrm{T}}}{(c_0 t_{\mathrm{w}})^4} \right]^{-1} V^{\mathrm{G}}(t) \tag{41}$$

in which $A^{\mathrm{T}} = |\boldsymbol{A}^{\mathrm{T}}|$, $A^{\mathrm{R}} = |\boldsymbol{A}^{\mathrm{R}}|$, and $c_0 t_{\mathrm{w}}$ represents the spatial extent of the exciting pulse. Combining (37) and (40) with (41), we obtain

$$\begin{aligned} V^{\mathrm{G}}_{\mathrm{norm}}(t) = & \Pi^{\mathrm{NF}}_{\mathrm{norm}}(\boldsymbol{\Xi}) \frac{S^{\mathrm{NF}}(t)}{4\pi |\boldsymbol{X}|^3_{\mathrm{norm}}} + \Pi^{\mathrm{IF}}_{\mathrm{norm}}(\boldsymbol{\Xi}) \frac{S^{\mathrm{IF}}(t)}{4\pi |\boldsymbol{X}|^2_{\mathrm{norm}}} \\ & + \Pi^{\mathrm{FF}}_{\mathrm{norm}}(\boldsymbol{\Xi}) \frac{S^{\mathrm{FF}}(t)}{4\pi |\boldsymbol{X}|_{\mathrm{norm}}} \end{aligned} \tag{42}$$

in which

$$\left\{ \Pi^{\mathrm{NF}}_{\mathrm{norm}}, \Pi^{\mathrm{IF}}_{\mathrm{norm}}, \Pi^{\mathrm{FF}}_{\mathrm{norm}} \right\}(\boldsymbol{\Xi}) = \left\{ D^{\mathrm{NF}}_{j,p}, D^{\mathrm{IF}}_{j,p}, D^{\mathrm{FF}}_{j,p} \right\}(\boldsymbol{\Xi}) \frac{A^{\mathrm{R}}_j A^{\mathrm{T}}_p}{A^{\mathrm{R}} A^{\mathrm{T}}} \tag{43}$$

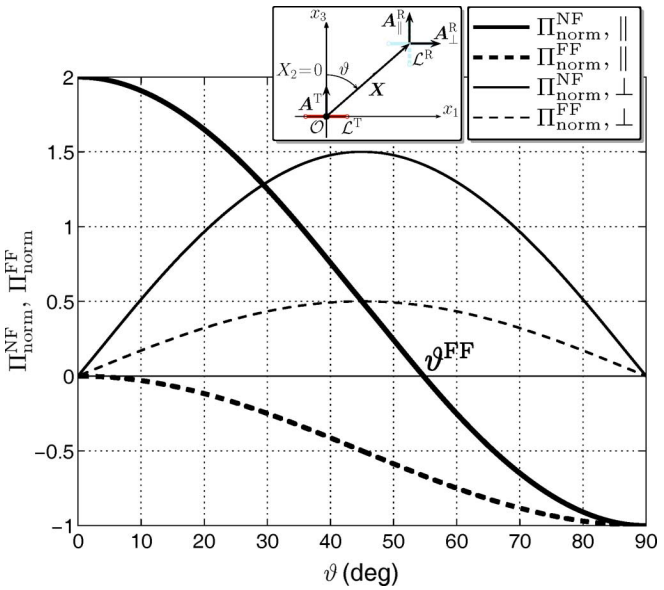


Fig. 6. The normalized projections $\Pi^{\rm NF}_{\rm norm}$ and $\Pi^{\rm FF}_{\rm norm}$ for $\boldsymbol{A}^{\rm R}\|\boldsymbol{A}^{\rm T}$ and $\boldsymbol{A}^{\rm R}\perp\boldsymbol{A}^{\rm T}$.

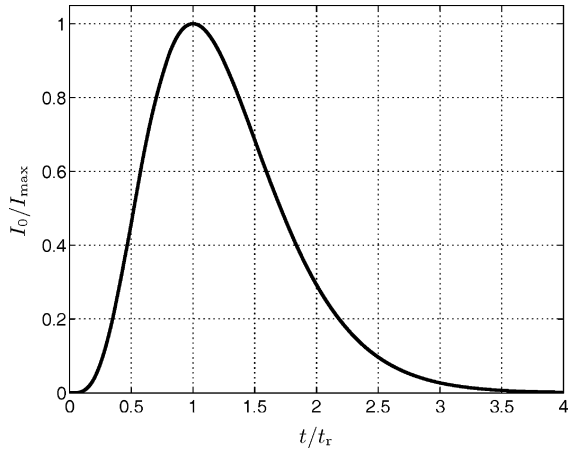


Fig. 7. The exciting power exponential electric current pulse for $\nu = 4$.

are the normalized projections of the wire-loop areas on the relevant direction characteristics, $|\boldsymbol{X}|_{\rm norm} = |\boldsymbol{X}|/(c_0 t_{\rm w})$ is the normalized inter-loop distance, and

$$S^{\rm NF}(t) = t_{\rm w}\partial_t I^{\rm T}(t)/I^{\rm T}_{\rm max} \tag{44}$$

$$S^{\rm IF}(t) = t^2_{\rm w}\partial^2_t I^{\rm T}(t)/I^{\rm T}_{\rm max} \tag{45}$$

$$S^{\rm FF}(t) = t^3_{\rm w}\partial^3_t I^{\rm T}(t)/I^{\rm T}_{\rm max} \tag{46}$$

are the normalized time signatures in the relevant regions. Evidently, in view of (38), $\Pi^{\rm NF}(\Xi) = \Pi^{\rm IF}(\Xi)$.

From (42) it follows that the pulse response can be factored into a *configurational constituent*, represented by the directional characteristics, together with the terms containing the normalized distance $|\boldsymbol{X}|_{\rm norm}$, and the *temporal constituents*, consisting of the time signatures.

Fig. 6 shows, for the two cases: $\boldsymbol{A}^{\rm R}||\boldsymbol{A}^{\rm T}$ ($\boldsymbol{A}^{\rm T} = A^{\rm T}\boldsymbol{i}_3$ and $\boldsymbol{A}^{\rm R} = A^{\rm R}\boldsymbol{i}_3$) and $\boldsymbol{A}^{\rm R} \perp \boldsymbol{A}^{\rm T}$ ($\boldsymbol{A}^{\rm T} = A^{\rm T}\boldsymbol{i}_3$ and $\boldsymbol{A}^{\rm R} = A^{\rm R}\boldsymbol{i}_1$), the directional characteristics as a function of the angle between

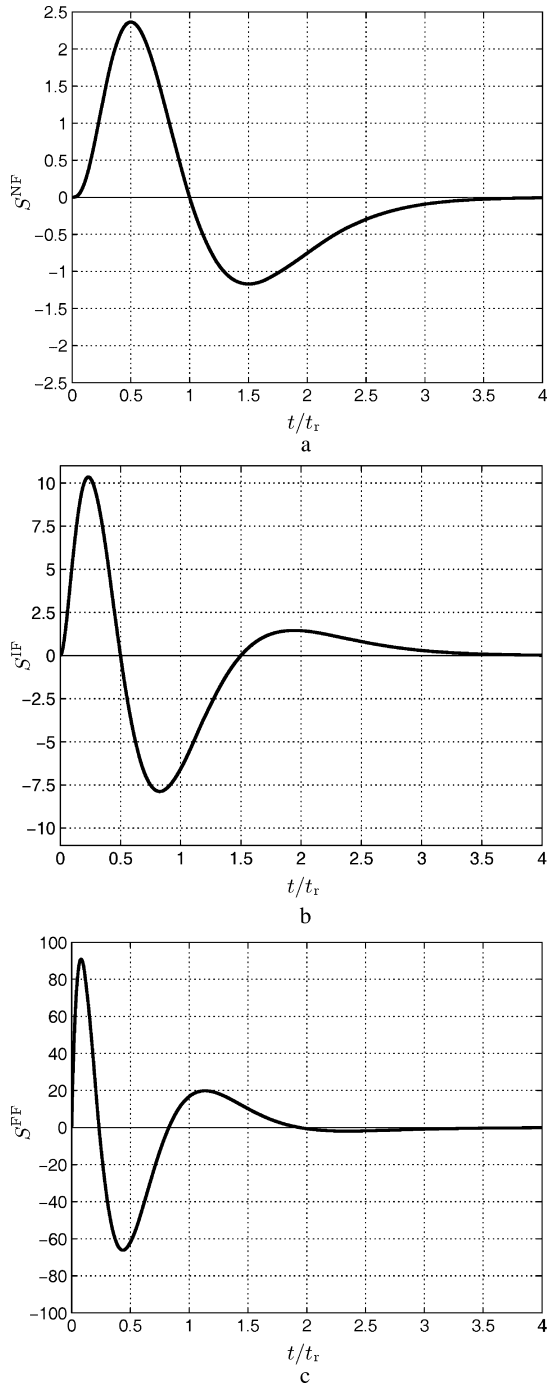


Fig. 8. The normalized time signatures in the different regions of the pulsed-field transfer between two small loops for the power exponential electric current pulse excitation shown in Fig. 7. (a) The near-field constituent $S^{\rm NF}$; (b) the intermediate-field constituent $S^{\rm IF}$; (c) the far-field constituent $S^{\rm FF}$.

$\boldsymbol{A}^{\rm T}$ and $\boldsymbol{X}$, with $\boldsymbol{X}$ in the $\{x_1, x_3\}$—plane. Note that $\Pi^{\rm NF}_{\rm norm}$ vanishes for $\vartheta = \vartheta^{\rm FF} = \arccos(3^{-1/2})$ in the case of the parallel orientation, while the other characteristics start from zero at $\vartheta = 0°$ and return to zero at $\vartheta = 90°$.

For the exciting electric current pulse we take the power exponential pulse with $\nu = 4$ (see Fig. 7). In this case, $t_{\rm w} \simeq 1.28 t_{\rm r}$. For a typical value of $t_{\rm r} = 100$ ps, we then have $t_{\rm w} \simeq 128$ ps which results into a spatial support of the pulse of size $c_0 t_{\rm w} = 38.4$ mm. Fig. 8 shows the normalized temporal constituents in

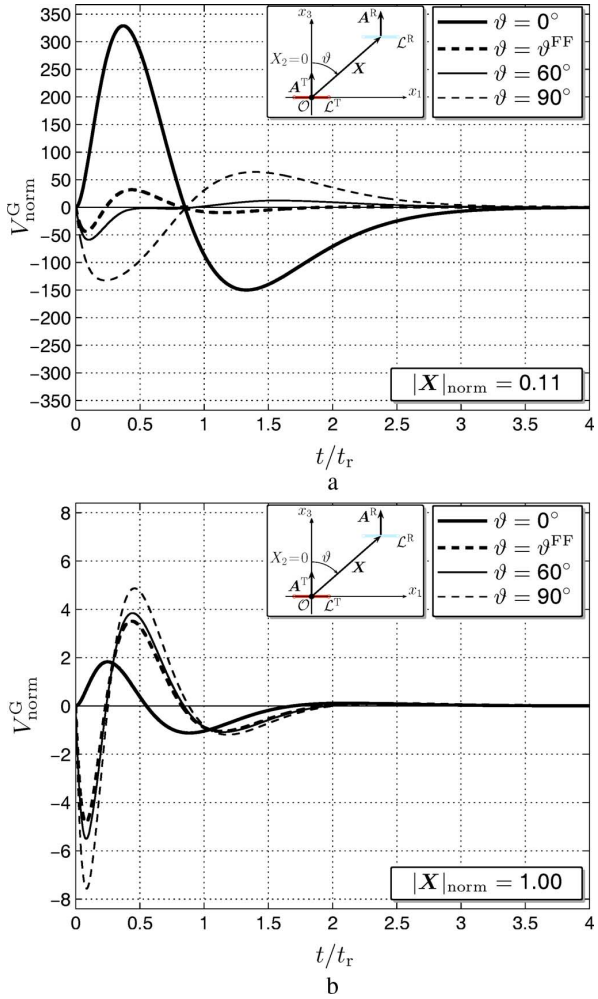


Fig. 9. The total field response in the pulsed-field transfer between two small loops for the power exponential electric current pulse excitation shown in Fig. 7. (a) Antenna response in the (predominantly) near-field region ($|\boldsymbol{X}|_{\mathrm{norm}} = 0.11$); (b) antenna response in the (predominantly) far-field region ($|\boldsymbol{X}|_{\mathrm{norm}} = 1$).

the three characteristic regions. They reflect the substantial effect of the increasing orders of differentiation on the signal amplitudes and pulse shapes. Fig. 9 shows, for the case $\boldsymbol{A}^{\mathrm{R}} \| \boldsymbol{A}^{\mathrm{T}}$, some pulse shapes of $V^{\mathrm{G}}_{\mathrm{norm}}(t)$ in the (predominantly) near-field region ($|\boldsymbol{X}|_{\mathrm{norm}} = 0.11$) and the (predominantly) far-field region ($|\boldsymbol{X}|_{\mathrm{norm}} = 1$) as a function of the included angle between $\boldsymbol{A}^{\mathrm{T}}$ and $\boldsymbol{X}$. Fig. 9(a) illustrates that, in the near-field region, the complete response changes significantly with $\vartheta$: it starts by having the largest value at $\vartheta = 0°$, ($S^{\mathrm{NF}}$ being the dominant constituent), at $\vartheta = \vartheta^{\mathrm{FF}}$ the near-field constituent vanishes and the signature of $S^{\mathrm{FF}}$ becomes visible, some influence of $S^{\mathrm{IF}}$ is noticeable at $\vartheta = 60°$, while at $\vartheta = 90°$, $S^{\mathrm{NF}}$ is dominant again, but has a reversed sign. In Fig. 9(b), the response is largely dominated by $S^{\mathrm{FF}}$, except at $\vartheta = 0°$ where, as shown by Fig. 6, $\Pi^{\mathrm{FF}}_{\mathrm{norm}}$ vanishes and the near-field $S^{\mathrm{NF}}$ constituent shows up.

An analysis of this kind has a wide applicability in the design of wireless communication systems (where, at reception, the signal related to the exciting current has to be reconstructed) and in the EM interference analysis of nanometer integrated circuits (where distorted pulse shapes can hamper the desired operation of the device). In all these cases, a detailed understanding of the pulsed-field transfer mechanism between two wire loops is an important building block.

Finally, it should be mentioned that the results constructed in this section can be considered as more detailed extensions of the ones discussed in [14], [15].

## X. Conclusion

Starting from the time-domain electromagnetic field reciprocity theorem of the time-convolution type, a direct time-domain approach is presented to construct the equivalent electric circuits describing the receiving properties of a multiport antenna system that is accessible via Kirchhoff circuit ports and upon which a pulsed electromagnetic field is incident. The analysis leads to novel and general Thévenin (voltage source, impedance based) and Norton (electric-current source, admittance based) circuit representations. The source strengths in these representations are expressed in terms of the field in which the antenna is placed, as the field is 'sensed' by the antenna's radiation properties in its transmitting state. In the case of the antenna placed in an incident plane wave, the sensing field is shown to be related to the antenna's far-field transmitted radiation characteristic in the direction from which the wave is incident. Applications to a typical indoor wireless communication environment and to the signal interpretation in the detection of the cosmic background radiation are briefly discussed. Numerical results are presented for the field transfer from a pulse-excited transmitting wire loop to some other receiving wire loop elsewhere in space, a configuration that is representative for the operation of wireless telecommunication systems and for the pulsed-field EM interference analysis in nano-electronic integrated circuit devices.

## Appendix A
## Generic Form of the Time-Domain Field Reciprocity Relation

The generic form of the field reciprocity relation applies to two admissible electromagnetic states, denoted by the superscripts A and B, respectively, present in one and the same bounded domain $\mathcal{D}$ in space. In each subdomain of $\mathcal{D}$ where the field quantities are continuously differentiable, they satisfy the Maxwell equations [4, Sec. 28.1]

$$\varepsilon_{k,m,p}\partial_m H_p^{\mathrm{A,B}} - \partial_t D_k^{\mathrm{A,B}} = J_k^{\mathrm{A,B}} \quad \text{for } \boldsymbol{x} \in \mathcal{D} \text{ and } t \in \mathbb{R} \tag{47}$$

$$\varepsilon_{j,n,q}\partial_n E_q^{\mathrm{A,B}} + \partial_t B_j^{\mathrm{A,B}} = -K_j^{\mathrm{A,B}} \quad \text{for } \boldsymbol{x} \in \mathcal{D} \text{ and } t \in \mathbb{R} \tag{48}$$

where:

| | |
|---|---|
| $E_q$ | electric field strength (V/m); |
| $H_p$ | magnetic field strength (A/m); |
| $D_k$ | electric flux density $(\mathrm{C/m^2})$; |
| $B_j$ | magnetic flux density (T); |
| $J_k$ | volume source density of external (active) electric current $(\mathrm{A/m^2})$; |

$K_j$ volume source density of external (active) magnetic current ($\mathrm{V/m^2}$);

$\varepsilon_{k,m,p}$ represents the completely antisymmetrical unit tensor of rank three (Levi-Civita tensor): $\varepsilon_{k,m,p} = 1$ for $\{k,m,p\} =$ even permutation of $\{1,2,3\}$, $\varepsilon_{k,m,p} = -1$ for $\{k,m,p\} =$ odd permutation of $\{1,2,3\}$, $\varepsilon_{k,m,p} = 0$ in all other cases.

The constitutive relations in the domain $\mathcal{D}$ are

$$D_k(\boldsymbol{x},t) = \eta_{k,q}(\boldsymbol{x},t) \overset{(t)}{*} E_q(\boldsymbol{x},t) \quad \text{for } \boldsymbol{x} \in \mathcal{D} \text{ and } t \in \mathbb{R} \tag{49}$$

$$B_j(\boldsymbol{x},t) = \zeta_{j,p}(\boldsymbol{x},t) \overset{(t)}{*} H_p(\boldsymbol{x},t) \quad \text{for } \boldsymbol{x} \in \mathcal{D} \text{ and } t \in \mathbb{R}. \tag{50}$$

In these relations, $\eta_{k,q}(\boldsymbol{x},t)$ represents the transverse admittance relaxation function per length of the medium, $\zeta_{j,p}(\boldsymbol{x},t)$ represents its longitudinal impedance relaxation function per length, and $\overset{(t)}{*}$ denotes time convolution. Both, $\eta_{k,q}$ and $\zeta_{j,p}$ are causal. It is emphasized that the uniqueness of the electromagnetic field initial-value problem can only be proven if the time Laplace transforms of these relaxation functions have a positive real part in the right half of the complex transform parameter plane [24], [25]. In the domain $\mathcal{D}^\infty$ outside $\mathcal{S}_0$, the constitutive relations are

$$D_k(\boldsymbol{x},t) = \epsilon_0 E_k(\boldsymbol{x},t) \quad \text{for } \boldsymbol{x} \in \mathcal{D}^\infty \text{ and } t \in \mathbb{R} \tag{51}$$

$$B_j(\boldsymbol{x},t) = \mu_0 H_j(\boldsymbol{x},t) \quad \text{for } \boldsymbol{x} \in \mathcal{D}^\infty \text{ and } t \in \mathbb{R} \tag{52}$$

where $\epsilon_0$ is the permittivity of free space and $\mu_0$ is the permeability of free space. Note that inside $\mathcal{S}_0$ the medium may be arbitrarily inhomogeneous and anisotropic, while it may show arbitrary loss mechanisms with their associated attenuation and dispersion. Across possible interfaces of jump discontinuities in material properties, the tangential components of $E_q$ and $H_p$ are continuous. At perfectly conducting surfaces, the tangential components of $E_q$ vanish.

The reciprocity relation of the time-convolution type [4, Section 28.2] interrelates two generic field states A and B defined in $\mathcal{D}$ by

$$\begin{aligned}
&\varepsilon_{k,m,p} \int_{\partial\mathcal{D}} \nu_k \left( E_m^{\mathrm{A}} \overset{(t)}{*} H_p^{\mathrm{B}} - E_m^{\mathrm{B}} \overset{(t)}{*} H_p^{\mathrm{A}} \right) \mathrm{d}A(\boldsymbol{x}) \\
&\quad = \int_{\mathcal{D}} \left\{ -\partial_t \left[ \left( \eta_{q,m}^{\mathrm{B}} - \eta_{m,q}^{\mathrm{A}} \right) \overset{(t)}{*} E_q^{\mathrm{A}} \overset{(t)}{*} E_m^{\mathrm{B}} \right] \right. \\
&\qquad \left. + \partial_t \left[ \left( \zeta_{r,p}^{\mathrm{B}} - \zeta_{p,r}^{\mathrm{A}} \right) \overset{(t)}{*} H_r^{\mathrm{A}} \overset{(t)}{*} H_p^{\mathrm{B}} \right] \right\} \mathrm{d}V(\boldsymbol{x}) \\
&\quad + \int_{\mathcal{D}} \left( J_q^{\mathrm{A}} \overset{(t)}{*} E_q^{\mathrm{B}} - K_r^{\mathrm{A}} \overset{(t)}{*} H_r^{\mathrm{B}} \right. \\
&\qquad \left. - J_m^{\mathrm{B}} \overset{(t)}{*} E_m^{\mathrm{A}} + K_p^{\mathrm{B}} \overset{(t)}{*} H_p^{\mathrm{A}} \right) \mathrm{d}V(\boldsymbol{x})
\end{aligned} \tag{53}$$

where $\partial\mathcal{D}$ denotes the boundary of the domain $\mathcal{D}$ and $\boldsymbol{\nu}$ is the unit vector along the outward normal to $\partial\mathcal{D}$. Note that the first term in the right-hand side of this relation vanishes when the media in States A and B are each others adjoints, i.e. if

$$\eta_{q,m}^{\mathrm{B}}(\boldsymbol{x},t) = \eta_{m,q}^{\mathrm{A}}(\boldsymbol{x},t) \quad \text{for } \boldsymbol{x} \in \mathcal{D} \text{ and } t \in \mathbb{R} \tag{54}$$

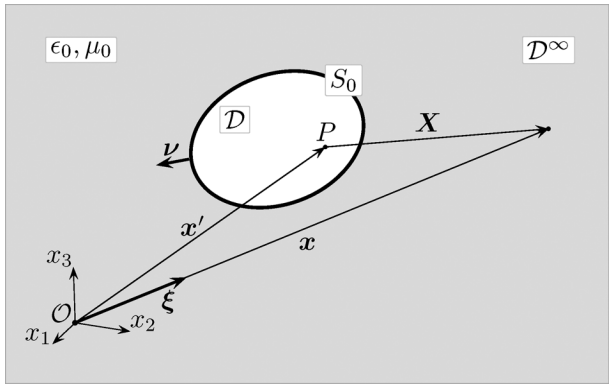


Fig. 10. Far-field approximation to the distance function from source point $\boldsymbol{x'} \in \mathcal{S}_0$ to observation point $\boldsymbol{x} \in \mathcal{R}^3 : |\boldsymbol{X}| = |\boldsymbol{x} - \boldsymbol{x'}| = |\boldsymbol{x}| - \xi_s x'_s + O|\boldsymbol{x}|^{-1}$ as $|\boldsymbol{x}| \to \infty$.

$$\zeta_{r,p}^{\mathrm{B}}(\boldsymbol{x},t) = \zeta_{p,r}^{\mathrm{A}}(\boldsymbol{x},t) \quad \text{for } \boldsymbol{x} \in \mathcal{D} \text{ and } t \in \mathbb{R} \tag{55}$$

whereas the second term vanishes when no sources are present inside $\mathcal{D}$. An important class of applications where (54) and (55) do not apply is the field of time-domain electromagnetic *inverse profiling* and *inverse scattering*. A survey of this kind of application is presented in [21].

## Appendix B
## The Time-Domain Far-Field Approximation in an Unbounded Exterior Domain

In the unbounded domain exterior to $\mathcal{S}_0$, the electromagnetic Green's tensors (point-source solutions) can be determined analytically [4, Sections 28.8 and 28.12]. From the corresponding Huygens surface source representations over the surface $\mathcal{S}_0$ it follows that the outgoing fields in $\mathcal{D}^\infty$ admit the far-field expansions

$$\begin{aligned}
\{E_q, H_p\}(\boldsymbol{x},t) = &\frac{\left\{E_q^\infty, H_p^\infty\right\}(\boldsymbol{\xi}, t - |\boldsymbol{x}|/c_0)}{4\pi|\boldsymbol{x}|} \\
&\times \left[1 + O\left(|\boldsymbol{x}|^{-1}\right)\right] \text{ as } |\boldsymbol{x}| \to \infty
\end{aligned} \tag{56}$$

where $\{E_q^\infty, H_p^\infty\}(\boldsymbol{\xi},t)$ are the electric-field and magnetic-field amplitude radiation characteristics of the antenna system and $\boldsymbol{\xi} = \boldsymbol{x}/|\boldsymbol{x}|$ is the unit vector in the direction of observation (see Fig. 10).

From substituting (56) in (47) and (48), combined with (51) and (52), it follows that

$$E_q^\infty = -(\mu_0/\epsilon_0)^{1/2} \varepsilon_{q,m,p} \xi_m H_p^\infty \tag{57}$$

$$H_p^\infty = (\epsilon_0/\mu_0)^{1/2} \varepsilon_{p,n,q} \xi_n E_q^\infty. \tag{58}$$

Upon taking $E_q^\infty$ as a reference for evaluating (57) and (58), this quantity follows by applying the expression (see [4])

$$E_q^\infty = \mu_0(\xi_q \xi_k - \delta_{q,k}) \partial_t A_k + \varepsilon_{q,n,j}(\xi_n/c_0) \partial_t F_j \tag{59}$$

where $\delta_{q,k}$ is the symmetrical unit tensor of rank two, and

$$A_k(\boldsymbol{\xi},t) = \int_{\boldsymbol{x'} \in \mathcal{S}_0} \varepsilon_{k,m,p} \nu_m H_p\left(\boldsymbol{x'}, t + \xi_s x'_s/c_0\right) \mathrm{d}A \tag{60}$$

$$F_j(\boldsymbol{\xi},t) = -\int_{\boldsymbol{x}'\in\mathcal{S}_0} \varepsilon_{j,n,q}\nu_n E_q\left(\boldsymbol{x}', t+\xi_s x'_s/c_0\right)\mathrm{d}A \quad (61)$$

with $\nu_m$ as the unit vector along the outward normal to $\mathcal{S}_0$, as indicated in Fig. 10. Note that the right-hand sides of (60) and (61) have the shape of a slant-stack, or Radon transform, discussed in [13].

## Appendix C
## The Receiving Antenna as a Scatterer in an Incident Field

In a variety of applications, a receiving antenna is placed in an incident field, the sources of which are either unknown or inaccessible. In principle, the field in the absence of the antenna is accessible to measurement. After the antenna has been placed in that field, the reciprocity theorem can be applied to the antenna's transmitting state (denoted by T) and the antenna's receiving state (denoted by R). The consequence of the placement of the antenna is that the field in the state R can be written as the superposition of the incident field prior to the placement (denoted by the superscript i) and the field scattered by the antenna (denoted by the superscript s), i.e.

$$\left\{E_q^{\mathrm{R}}, H_p^{\mathrm{R}}\right\} = \left\{E_q^{\mathrm{i}} + E_q^{\mathrm{s}}, H_p^{\mathrm{i}} + H_p^{\mathrm{s}}\right\}. \quad (62)$$

The reciprocity relation (53) is now applied to a domain bounded internally by $\mathcal{S}_1$ (the termination of the antenna system, on which this system terminates into its accessible ports) and externally by a surface $\partial\mathcal{D}$ in $\mathcal{D}^\infty$ that completely encloses $\mathcal{S}_1$. Note that representations of the type (57) and (58) hold on $\partial\mathcal{D}$ for both the field in the transmitting state and the scattered field in the receiving state and that both these quantities are outgoing fields on $\partial\mathcal{D}$. Upon taking the domain in between $\mathcal{S}_1$ and $\partial\mathcal{D}$ to be source free and the media inside it to be the each others' adjoints in the transmitting and the receiving states, we obtain the identity needed for the scattering description

$$\varepsilon_{k,m,p}\int_{\mathcal{S}_1}\nu_k\left(E_m^{\mathrm{T}} \overset{(t)}{*} H_p^{\mathrm{R}} - E_m^{\mathrm{R}} \overset{(t)}{*} H_p^{\mathrm{T}}\right)\mathrm{d}A(\boldsymbol{x}) = \varepsilon_{k,m,p}\int_{\partial\mathcal{D}}\nu_k\left(E_m^{\mathrm{T}} \overset{(t)}{*} H_p^{\mathrm{i}} - E_m^{\mathrm{i}} \overset{(t)}{*} H_p^{\mathrm{T}}\right)\mathrm{d}A(\boldsymbol{x}). \quad (63)$$

## Appendix D
## Interfacing the Multiport Kirchhoff-Type Antenna System With the Field Description

Let a local part of the antenna system occupy a bounded domain in space of such relatively small dimensions that the travel times of electromagnetic waves to traverse this domain is negligible with respect to the pulse time widths of the information carrying fields in and around them. Let, further this part be accessible at a number $N_{\mathrm{ports}}$ Kirchhoff ports. The surface integral in the reciprocity relation (53) is then expressible in terms of the voltages $\{V_M(t); M = 1,\ldots,N_{\mathrm{ports}}\}$ across and the electric currents $\{I_N(t); N = 1,\ldots,N_{\mathrm{ports}}\}$ fed into the $N_{\mathrm{ports}} \geqslant 1$ that serve to characterize the electric or electronic system behavior of the interior. Analysis of the local fields by expressing the electric field strength as the (opposite of) the gradient of potential leads to the relevant link

$$\varepsilon_{k,m,p}\int_{\mathcal{S}_1}\nu_k\left(E_m^{\mathrm{A}} \overset{(t)}{*} H_p^{\mathrm{B}} - E_m^{\mathrm{B}} \overset{(t)}{*} H_p^{\mathrm{A}}\right)\mathrm{d}A(\boldsymbol{x}) = \sum_{M=1}^{N_{\mathrm{ports}}}\left[V_M^{\mathrm{A}}(t) \overset{(t)}{*} I_M^{\mathrm{B}}(t) - V_M^{\mathrm{B}}(t) \overset{(t)}{*} I_M^{\mathrm{A}}(t)\right] \quad (64)$$

where the electric currents are oriented along $\nu_k$.

## Acknowledgment

The authors would like to express their thanks to the reviewers for their careful reading of the manuscript and their constructive suggestions for the improvement of the paper.

The research reported in this paper was partially carried out during an internship V. Tomassetti had effectuated at the International Research Centre for Telecommunications and Radar (IRCTR) under the auspices of the European Community action programme in the field of education ERASMUS.

## References

[1] H. A. Lorentz, "The theorem of Poynting concerning the energy in the electromagnetic field and two general propositions concerning the propagation of light," *Versl. Kon. Akad. Wetensch. Amsterdam*, vol. 4, p. 176, 1896.
[2] J. van Bladel, *Electromagnetic Fields*, 2nd ed. Hoboken: Wiley, 2007.
[3] R. E. Collin, *Field Theory of Guided Waves*, 2nd ed. New York: Wiley.
[4] A. T. de Hoop, *Handbook of Radiation and Scattering of Waves*. London: Academic Press, 1995.
[5] R. E. Collin, "Limitations on the Thévenin and Norton equivalent circuits for a receiving antenna," *IEEE Antennas Propag. Mag.*, vol. 45, pp. 119–124, April 2003.
[6] R. E. Collin, "Remarks on "Comments on limitations on the Thévenin and Norton equivalent circuits for a receiving antenna"," *IEEE Antennas Propag. Mag.*, vol. 45, pp. 99–100, Aug. 2003.
[7] A. W. Love, "Comment: "On the equivalent circuit of a receiving antenna"," *IEEE Antennas Propag. Mag.*, vol. 44, pp. 124–125, Oct. 2002.
[8] A. W. Love, "Comment on "Limitations of the Thévenin and Norton equivalent circuits for a receiving antenna"," *IEEE Antennas Propag. Mag.*, vol. 45, pp. 98–99, Aug. 2003.
[9] S. V. Savov, "An optimization of a voltage pulse excitation in a UWB radio system," *IEEE Trans. Antennas Propag.*, vol. 55, pp. 139–142, Jan. 2007.
[10] R. A. Scholtz, D. M. Pozar, and W. Namgoong, "Ultra-wideband radio," *EURASIP J. Appl. Signal Process.*, vol. 3, pp. 252–272, Jun. 2005.
[11] G. S. Smith, "A direct derivation of a single-antenna reciprocity relation for the time domain," *IEEE Trans. Antennas Propag.*, vol. 52, pp. 1568–1577, Jun. 2004.
[12] D. M. Pozar, R. E. McIntosh, and S. G. Walker, "The optimum feed voltage for a dipole antenna for pulse radiation," *IEEE Trans. Antennas Propag.*, vol. AP-31, pp. 563–569, Jul. 1983.
[13] A. Shlivinski, E. Heyman, and R. Kastner, "Antenna characterization in the time domain," *IEEE Trans. Antennas Propag.*, vol. 45, pp. 1140–1148, Jul. 1997.
[14] C. E. Baum, "General properties of antennas," *Sensor and Simulation Notes*, Jul. 23, 1991, Note 330, Philips Lab., Kirkland AFB, NM.
[15] C. E. Baum, "General properties of antennas," *IEEE Trans. Electromagn. Compat.*, vol. 44, pp. 18–24, Feb. 2002.
[16] A. T. de Hoop, "The $N$-port receiving antenna and its equivalent electrical network," *Philips Res. Repts.*, vol. 30, pp. 302–315, 1975.
[17] Y. W. Lee, *Statistical Theory of Communication*. New York: Wiley, 1960.

[18] K. Mandke, H. Nam, L. Yerramneni, C. Zuniga, and T. Rappaport, "The evolution of ultra wide band radio for wireless personal area networks," *High Frequency Electron*, vol. 2, Sep. 2003 [Online]. Available: http://www.highfrequencyelectronics.com

[19] D. Porcino and W. Hirt, "Ultra-wideband radio technology: Potential and challenges ahead," *IEEE Commun. Soc. Mag.*, vol. 41, pp. 66–74, Jul. 2003.

[20] A. C. S. Readhead, S. T. Myers, T. J. Pearson, J. L. Sievers, B. S. Mason, C. R. Contaldi, J. R. Bond, R. Bustos, P. Altamirano, C. Achermann, L. Bronfman, J. E. Carlstrom, J. K. Cartwright, S. Casassus, C. Dickinson, W. L. Holzapfel, J. M. Kovac, E. M. Leitch, J. May, S. Padin, D. Pogosyan, M. Pospieszalski, C. Pryke, R. Reeves, M. C. Shepherd, and S. Torres, "Polarization observations with the cosmic background imager," *Science*, vol. 306, pp. 836–844, Oct. 2004.

[21] M. L. Oristaglio and T. M. Habashy, "Some uses (and abuses) of reciprocity in wavefield inversion," in *Wavefields and Reciprocity. Proc. Symp. Held in Honor of Prof. Dr. A. T. de Hoop* , Delft, The Netherlands, Nov. 20–21, 1996, pp. 1–22.

[22] S. Padin, J. K. Cartwright, B. S. Mason, T. J. Pearson, A. C. S. Readhead, M. C. Shepherd, J. Sievers, P. S. Udomprasert, W. L. Holzapfel, S. T. Myers, J. E. Carlstrom, E. M. Leitch, M. Joy, L. Bronfman, and J. May, "First intrinsic anisotropy observations with the cosmic background imager," *Astrophys. J. Lett.*, vol. 549, pp. L1–L5, Mar. 2001.

[23] D. Quak, "Analysis of transient radiation of a (traveling) current pulse on a straight wire segment," in *Proc. IEEE EMC Int. Symp.*, Aug. 2001, vol. 2, pp. 849–854.

[24] A. T. de Hoop, "Time-domain reciprocity theorems for electromagnetic fields in dispersive media," *Radio Sci.*, vol. 22, no. 7, pp. 1171–1178, Dec. 1987.

[25] A. T. de Hoop, "A time-domain uniqueness theorem for electromagnetic wavefeld modeling in dispersive, anisotropic media," *URSI—Radio Sci. Bulletin*, no. 305, pp. 17–21, Jun. 2003.

[26] *H. A. Lorentz Collected Papers*, P. Zeeman and D. Fokker, Eds. The Hague, The Netherlands: Martinus Nijhoff, 1936, vol. III, pp. 1–11.

[27] J. van Bladel, *Electromagnetic Fields*. New York: McGraw-Hill, 1964, 1st print.

[28] R. E. Collin, *Field Theory of Guided Waves*. New York: McGraw-Hill, 1960, 1st print.

**Adrianus T. de Hoop** (M'00) was born in Rotterdam, the Netherlands, on December 24, 1927. He received the M.Sc. degree in electrical engineering in 1950 and the Ph.D. degree in the technological sciences in 1959 from Delft University of Technology, Delft, The Netherlands, both with the highest distinction.

He served Delft University of Technology as an Assistant Professor from 1950 to 1957, Associate Professor from 1957 to 1960, and Full Professor in electromagnetic theory and applied mathematics from 1960 to 1996, and since 1996, he has been the Lorentz Chair Emeritus Professor in the Faculty of Electrical Engineering, Mathematics and Computer Science. In 1970, he founded the Laboratory of Electromagnetic Research at Delft University of Technology which has developed into a world-class center for electromagnetics. His research interests are in the broad area of wavefield modeling in acoustics, electromagnetics and elastodynamics. His interdisciplinary insights and methods in this field can be found in his *Handbook of Radiation and Scattering of Waves* (London, Academic Press, 1995), with wavefield reciprocity serving as one of the unifying principles governing direct and inverse scattering problems and wave propagation in complex (anisotropic and dispersive) media. From 1956 to 1957, he was a Research Assistant with the Institute of Geophysics, University of California at Los Angeles, where he pioneered a modification of the Cagniard technique for calculating impulsive wave propagation in layered media, later to be known as the "Cagniard-De-Hoop technique." On a regular basis, since 1982, he a Visiting Scientist with Schlumberger-Doll Research, Ridgefield, CT (presently at Cambridge, MA), where he contributes to research on geophysical applications of acoustic, electromagnetic and elastodynamic waves. Recently, he is exploring a method for computing pulsed electromagnetic fields in strongly heterogeneous media with application to (micro- or nano-scale) integrated circuits.

Dr. De Hoop is a Member of the Royal Netherlands Academy of Arts and Sciences and a Foreign Member of the Royal Flemish Academy of Belgium for Science and Arts. He holds an Honorary Doctorate in the Applied Sciences from Ghent University, Belgium (1981). Grants from the "Stichting Fund for Science, Technology and Research" (founded by Schlumberger Limited) supported his research at Delft University of Technology. He was awarded the 1989 Research Medal of the Royal Institute of Engineers in The Netherlands, the IEEE 2001 Heinrich Hertz Gold Research Medal, and the 2002 URSI (International Scientific Radio Union) Balthasar van der Pol Gold Research Medal. In 2003, Her Majesty the Queen of The Netherlands decorated him "Knight in the Order of the Netherlands Lion."

**Ioan E. Lager** (M'02) was born in Braşov, Romania, on September 26, 1962. He received the M.Sc. and Ph.D. degrees in electrical engineering from the "Transilvania" University of Braşov, Braşov, Romania, in 1987 and in 1998, respectively, and the Ph.D. degree in electrical engineering from Delft University of Technology, Delft, The Netherlands, in 1996.

He successively occupied several research and academic positions with the "Transilvania" University of Braşov and the Delft University of Technology, where he is currently an Associate Professor, since 2008, with the IRCTR. In 1997, he was a Visiting Scientist with Schlumberger-Doll Research, Ridgefield, CT. He coordinates the "Applied Electromagnetics" sector of IRCTR, a group of scientists and technicians involved in establishing a bridge between electromagnetic field theory and the design, implementation and physical measurement of radio-frequency front-end architectures. His research interests cover computational electromagnetics and antenna engineering, with an emphasis on non-periodic (interleaved) array antenna architectures.

**Valerio Tomassetti** was born in Fermo, Italy, on August 14, 1981. He received the M.Sc. degree in electronic engineering from the University of Perugia, Italy, in 2007. His thesis was based on research undergone at the IRCTR Group, Technical University of Delft, The Netherlands, during a six month ERASMUS student exchange programme.

He is currently working on an Interuniversitary Master degree in nanotechnologies organized by the Interuniversitary Coordination for Nanotechnologies in Veneto (CIVEN), Venice, Italy.